doi:10.3772/j.issn.1006-6748.2024.01.008

A novel DPSS filter optimization scheme to reduce the intrinsic interference of FBMC-QAM systems①

DONG Qiyang(董琪阳), MA Tianming②, JIN Jie, WU Zhong
(School of Electrical and Electronic Engineering, Shanghai University of Engineering Science, Shanghai 201620, P. R. China)

Abstract

In order to reduce the intrinsic interference of the filter bank multicarrier-quadrature amplitude modulation (FBMC-QAM) system, a novel filter optimization scheme based on discrete prolate spheroidal sequences (DPSS) is proposed. Firstly, a prototype filter function based on DPSS is designed, since the eigenvalue can be used as an indicator of the energy concentration of DPSS, so a threshold is set, and the sequence with the most concentrated energy is selected under the threshold, that is, the sequence with the eigenvalue higher than the threshold, and the prototype filter function is rewritten as a weighted sum function of multiple eigenvectors. Under the energy constraints of the filter, the relationship between the eigenvectors and the intrinsic interference function is established, and the function problem is transformed into an optimization problem for the weighted coefficients. Through the interior point method, the most suitable weight is found to obtain the minimum intrinsic interference result. Theoretical analysis and simulation results show that compared with the prototype filters such as Type1 and CaseC, the DPSS filter applying the proposed optimization algorithm can effectively suppress the intrinsic interference of the system and obtain a better bit error rate (BER) performance.

Key words: filter bank multicarrier-quadrature amplitude modulation (FBMC-QAM), intrinsic interference, discrete prolate spheroidal sequences (DPSS), interior point method

0 Introduction

The 4th-generation mobile communication technology (4G) adopts orthogonal frequency division multiplexing (OFDM) technology, which requires cyclic prefix (CP) to reduce the inter-symbol interference (ISI)[1], which leads to the reduction of spectral efficiency, so scholars have been trying to optimize the waveform selection in the 5th-generation mobile communication technology (5G), thus the filter bank multicarrier (FBMC) technique was developed[2]. The FBMC system is composed of an analysis filter bank (AFB) and a synthesis filter bank (SFB), which are modulated and demodulated by dedicated prototype filters instead of the rectangular filters used in OFDM, which not only greatly reduce the out-of-band emissions (OOBE), but also further improve the spectral efficiency by discarding the CP[3].

Conventional FBMC systems apply offset quadrature amplitude modulation (OQAM), which transmits the imaginary and real parts of the data signal separately that differ by one-half unit time, thus ensuring quadrature in the real domain[4]. However, OQAM only turns the interference into pure imaginary numbers but cannot eliminate it completely. In addition, OQAM itself expresses poor compatibility with the conventional 4G technologies such as multiple-input multiple-output (MIMO), so scholars began to consider adopting the traditional OFDM quadrature amplitude modulation (QAM) instead of OQAM to improve the compatibility with MIMO[5]. A major issue that needs to be addressed before FBMC-QAM is practical application is how to effectively suppress intrinsic interference in actual communication. The existing FBMC-QAM scheme can only eliminate the intrinsic interference in conventional FBMC-OQAM in ideal channels. The NDPSS filter proposed in this paper can effectively suppress the

① Supported by the National Natural Science Foundation of China (No. 61601296, 61201244), the Science and Technology Innovation Action Plan Project of Shanghai Science and Technology Commission (No. 20511103500), and the Talent Program of Shanghai University of Engineering Science (No. 2018RC43).

② To whom correspondence should be addressed. E-mail: tmma@sues.edu.cn.

Received on Mar. 21, 2023

intrinsic interference of FBMC-QAM in actual wireless mobile communication channels by optimizing the design scheme of the prototype filter.

For FBMC-QAM systems, the design of the prototype filter is the core of performance improvement, which can be divided into two types: direct design method and indirect design method[6]. The direct design method is to solve the coefficients of the prototype filter directly, select the desired evaluation index, construct the objective function, and optimize the parameters affecting the evaluation index. The indirect design method includes the frequency sampling method and the window function method to design the filter in the frequency and time domains, respectively. In Ref. [7], a pair of prototype filters was designed using the frequency domain sampling method, dividing the input signals into odd and even groups, transmitting them respectively, and determining the structured parameters of the odd-even filter according to the four pairs of orthogonal relations that the prototype filter groups need to satisfy. Ref. [8] proposed a prototype filter named Type1, which was designed based on the minimization ISI, while Ref. [9] designed a prototype filter CaseC by minimizing the signal interference ratio under the constraints of the decay rate and the discrete ones through a global optimization algorithm.

Ref. [10] proposed an application of discrete prolate spheroidal sequences (DPSS) on discrete time functions, which is more advantageous than the traditional orthogonal expansion for discontinuous functions. In this paper, an NDPSS filter optimization algorithm is proposed, which applies the interior point method to find the most suitable weights and can further improve the bit error rate (BER) performance of the system while effectively reducing the intrinsic interference of the FBMC-QAM system. This optimization of the design scheme of the prototype filter by the indirect design method reduces the design complexity. With the performance advantages of discrete prolate spheroidal sequences energy concentration of 1, the parameters of the filter are better optimized in the iterative process. The filter design scheme in the Refs [8,9] fixes the parameters after an iterative optimization, but the design scheme in this paper is optimized by optimizing the parameters after each iteration through the internal point method so that after each iteration, so the system's bit error rate performance get better improved. Compared with the OFDM system used in 4G, the FBMC-QAM proposed in this paper also adopts QAM modulation, which can be better compatible with existing hardware devices. The difference is that the filter used in OFDM is a rectangular filter and requires cyclic prefix, while the filter proposed in this paper is redesigned indirectly on the basis of discrete prolate spheroidal sequences and does not require cyclic prefix.

1 FBMC-QAM system model

The transmitter model of FBMC-QAM system is illustrated in Fig. 1. Assume that the nth symbol on the kth subcarrier of the FBMC system transmitter is $d_{k,n}$, after QAM modulation and serial-parallel conversion, the baseband transmit signal at time t can be expressed as[11]

$$y(t) = \sum_{n} \sum_{k=0}^{M-1} d_{k,n} g(t - nT) e^{j2\pi Fkt} \tag{1}$$

where M is the number of carriers, $g(t)$ is the prototype filter, and F is the subcarrier frequency interval.

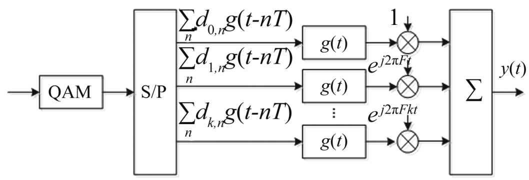

Fig. 1 Block diagram of transmitter structure of FBMC-QAM system

Assume that only the impact of additive white Gaussian noise (AWGN) in the channel is considered, the signal received at the receiver end of the system can be expressed as

$$r(t) = y(t) + n(t) \tag{2}$$

where $n(t)$ is AWGN. After passing AFB, $r(t)$ can be expressed as

$$\begin{aligned} d_{k,n} &= \int_{-\infty}^{\infty} r(t) g^*(t - nT) e^{-j2\pi Fkt} \mathrm{d}t \\ &= \sum_{n'} \sum_{k=0}^{M-1} d_{k,n} \int_{-\infty}^{\infty} g(t - nT) g^*(t - nT) \\ &\quad e^{-j2\pi F(k-k')t} \mathrm{d}t + n_{k,n} \\ &= d_{k,n} + I_{k,n} + n_{k,n} \end{aligned} \tag{3}$$

where * is the complex conjugate, $d_{k,n}$ is the useful signal, $I_{k,n}$ is the intrinsic interference, and $n_{k,n}$ is the noise, which can be respectively expressed as

$$I_{k,n} = \sum_{(k,n) \neq (k',n')} d_{k,n} \int_{-\infty}^{\infty} g(t - n'T) g^*(t - nT) e^{-j2\pi F(k-k')t} \mathrm{d}t \tag{4}$$

$$n_{k,n} = \int_{-\infty}^{\infty} n(t) g^*(t - nT) e^{-j2\pi Fkt} \mathrm{d}t \tag{5}$$

According to the fuzzy function defined in Ref. [12], $A_g(T_0, F_0)$ can be defined as

$$A_g(T_0, F_0) = \int_{-\infty}^{\infty} g(t) g^*(t - T_0) e^{-j2\pi F_0 t} \mathrm{d}t \tag{6}$$

Assume that $\Delta n = n - n'$ and $\Delta k = k - k'$, then Eq. (4) can be further expressed as

$$I_{k,n} = \sum_{(k,n)\neq(k',n')} d_{k,n} \int_{-\infty}^{\infty} g(t-(n-\Delta n)T) g^* (t-nT) e^{-j2\pi F\Delta k t} \mathrm{d}t$$
$$= \sum_{(k,n)\neq(k',n')} d_{k,n} A_g(\Delta n, \Delta k) \quad (7)$$

Fig. 2 depicts a plot of the fuzziness function of the sinusoidal signal with respect to time delay and frequency shift, from which it can be seen that all points except the center point $(\Delta k, \Delta n) = (0,0)$ will be used to calculate the intrinsic interference coefficient of the system.

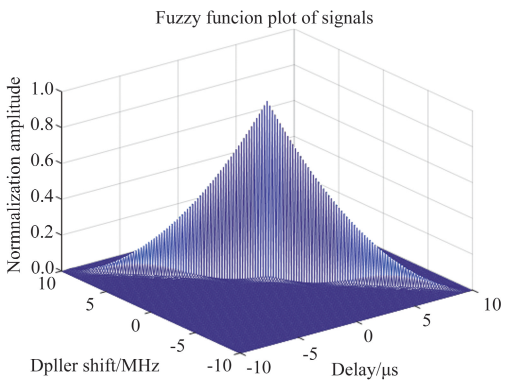

Fig. 2 Fuzzy function of time shift and frequency offset

The intrinsic interference coefficient can be defined as

$$\Gamma_{\Delta n,\Delta k} = A_g(\Delta n, \Delta k) \quad (8)$$

Thus Eq. (7) can be further expressed as

$$I_{k,n} = \sum_{(k',n')\neq(k,n)} d_{k',n} \Gamma_{\Delta n,\Delta k} \quad (9)$$

According to Eq. (9), it is easy to see that when $(k', n') \neq (k, n)$, the interference mainly comes from the nearby signals (k', n').

2 Discrete long spherical sequences

In digital communication systems, the problem of simultaneously limiting signals in both the time and frequency domains has been a hot research topic. The energy concentration level of a signal can be expressed as[13]

$$P = \frac{\int_{-T_0}^{T_0} |g(t)|^2 \mathrm{d}t}{\int_{-\infty}^{\infty} |g(t)|^2 \mathrm{d}t} \quad (10)$$

If $g(t)$ can strictly limit the time in the interval $[-T_0, T_0]$, then P will reach a maximum value of 1. Since time and frequency are negatively correlated, the Fourier transform of a time-limited function is equal to an infinitely wide bandwidth.

The problem of time and frequency concentration is how to make P maximized while keeping $g(t)$ as the limiting bandwidth. In this regard, a set of band-limited functions $\Psi(t,b)$ are proposed in Ref. [5], which can be maximally concentrated in a given time interval. These functions can be called prolate spheroidal wave functions (PSWFs) or Slepian functions[14], which are based on the angular solution $S_{0p}(b,t)$ and the radial solution $R_{0p}(b,1)$ of the Helmholtz fluctuation equation for the first class of spherical coordinate systems and can be expressed as[15]

$$\Psi(t,b) = \frac{\sqrt{\lambda_p(b)/T_0}}{\sqrt{\int_{-1}^{1} S_{0p}^2(b,t)\mathrm{d}t}} S_{0p}(b, t/T_0) \quad (11)$$

where,

$$\lambda_p(b) = \frac{2b}{\pi} R_{0p}^2(b,1) \quad (12)$$

According to Eq. (11), it is easy to discover that $\Psi(t,b)$ not only depends on the parameters of t and b but also on the time T_0 and the function order p, where $b = T_0 B/2$ and B is a given p-order bandwidth of $\Psi(t,b)$.

According to Ref. [16], the concentration degree of $\Psi(t,b)$ in $[-T_0, T_0]$ can be expressed as

$$\int_{-T_0}^{T_0} \frac{\sin[\pi(x-t)B]}{\pi(x-t)} \Psi(t,b)\mathrm{d}t = \lambda_p(b)\Psi_p(x,b) \quad (13)$$

where $\sin[\pi(x-t)B]/[\pi(x-t)]$ is a sinc function and can be viewed as a symmetric Toeplitz operator kernel; $\lambda_p(b)$ is the eigenvalue of the sinc function kernel, which is also an indicator of the energy concentration of the interval $[-T_0, T_0]$. If $\lambda_0(b)$ is the largest eigenvalue in Eq. (12), then its corresponding eigenfunction $\Psi_0(t,b)$ is usually referred to as the Slepian window[17] on the continuous time domain.

Moreover, for a given time interval $2T_0$, there are L samples and for each $p = 0, 1, 2, \ldots, L-1$, the Slepian window defines $\phi_c^{(p)}(L,B)$ as the solution of the equation[17]

$$\sum_{l=0}^{L-1} \frac{\sin[\pi(c-l)B]}{\pi(c-l)} \phi_l^{(p)}(L,B) = \lambda_p(L,B)\phi_c^{(p)}(L,B) \quad (14)$$

where $c \in Z$, and $\lambda_p(L,B)$ is the eigenvalue of the sinc function. By restricting $\phi_c^{(p)}(L,B)$ to $c \in \{0, L$

$-1\}$, the sequence $\phi^{(0)}(L,B)$ is the only time-constrained and the most frequency-concentrated sequence under such conditions, and $\phi^{(1)}(L,B)$ is the second most energy-concentrated sequence of the DPSS which is orthogonal to $\phi^{(0)}(L,B)$ [10]. Therefore, Eq. (13) can be re-expressed as

$$\boldsymbol{Q}(L,B)\phi^{(p)}(L,B) = \lambda(L,B)\phi^{(p)}(L,B) \tag{15}$$

These sequences are the eigenvectors of the $L \times L$ matrix $\boldsymbol{Q}(L,B)$, where

$$\boldsymbol{Q}(L,B)_{l,c} = \frac{\sin[\pi(c-l)B]}{\pi(c-l)}$$
$$0 \leqslant l \leqslant L-1,\ 0 \leqslant c \leqslant L-1 \tag{16}$$

3 NDPSS prototype filter optimization design

For a given filter length and bandwidth, the first extended sequence of DPSS $\phi^{(0)}(L,B)$ is defined as the eigenvector corresponding to the maximum eigenvalue of the matrix $\boldsymbol{Q}(L,B)$, which provides the optimal frequency-focused pulse. In view of the good properties of DPSS, a new DPSS (NDPSS) prototype filter is proposed, which minimizes the intrinsic interference of the FBMC-QAM system by limiting the time-frequency parameters of DPSS using fuzzy functions.

Firstly, a function is designed by using the prototype filter required for DPSS, since the eigenvalues are the indicators of the energy concentration of DPSS, therefore, select the eigenvectors $\phi^{(p)}(L_g,B)$ in the matrix $\boldsymbol{Q}(L,B)$ with eigenvalues $\lambda_p(L_g,B)$ above a certain threshold γ. The first eigenvalue has a strong energy concentration, which is very close to 1, while the others are close to 0. By this process, for a given bandwidth B, the sequence with the highest energy concentration $\phi^{(p)}(L_g,B)$ is selected. Finally, the proposed prototype filter can be described as a weighted sum of N_e sequences

$$g = \sum_{p=0}^{N_e-1} w_p \phi^{(p)}(L_g,B) \tag{17}$$

where $w_p(p=0,1,\ldots,N_e-1)$ is the optimal weight and $g=[g(0),g(1),\ldots,g(L_g-1)]$ is the discrete response of $g(t)$ at $g(m)=\mathrm{g}(mT/M)$.

Based on the definition of the ideal prototype filter in Eq. (17) and considering the system intrinsic interference described in Eq. (7), an optimization model is proposed to find the optimal prototype filter of the FBMC-QAM system. Its main purpose is to find the optimal weight w_p of the prototype filter which minimizes the energy of intrinsic interference coefficient $\Gamma_{\Delta n,\Delta k}$ under the filter energy constraint, thus the optimization problem can be formulated as

$$\min_{\omega} \sum_{(k',n')\neq(k,n)} \left| \sum_m g(m-n'M)g^*(m-nM)e^{-j\frac{2\pi\Delta_k m}{M}} \right|^2$$
$$\text{s.t.} \quad g^{\mathrm{H}}g = 1 \tag{18}$$

To solve the above optimization problem, the interior point method[17] is adopted, which ensures that there are different random initial weights w each time during several optimization processes, and then selects the best one, which is the minimum result of the disturbance. The whole process of it can be described by the pseudo-code shown in Algorithm 1.

Algorithm 1 NDPSS filter optimization algorithm based on the interior point method

procedure filter design $(L_g, B, i_{\max})$
$interf_{\min} \leftarrow \infty$
Calculate $Q(L_g,B)$
Select eigenvalues greater than γ
Select the eigenvector $\phi^{(p)}(L_g,B)$ corresponding to this eigenvalue
for $i = 1$ to $i_{\max}$
$w \quad CN(0,1)$
$w \leftarrow w/\|w\|$
Calculate g according to Eq. (17)
$interf = \sum_{(k',n')\neq(k,n)} |\Gamma|_{\Delta n,\Delta k}^2$
if $interf < interf_{\min}$ then
$interf_{\min} \leftarrow interf$
$g_{\mathrm{opt}} \leftarrow g$
end if
end for
return g_{opt}
end procedure

4 Performance simulation analysis

For a given FBMC-QAM system, its simulation parameters are shown in Table 1. In view of the time-varying characteristics of the actual 5G mobile communication channels, ITU-VB[18] is applied as the channel model for the system simulation.

Suppose the threshold in Algorithm 1 is $\gamma = 0.99$ and the iterative interference cancellation (IIC) method proposed in Ref. [19] is applied to compare the BER performance of NDPSS with other prototype filters under the same bandwidth.

Firstly, compare NDPSS with Type1 in Ref. [8] and CaseC in Ref. [9]. Suppose $B=4$ and $N_e=3$, therefore $p=0,1,2$, and for NDPSS it needs to optimize 3 parameters. Although they have the same bandwidth, their energy distribution is different, the main reason lies in the fact that the purpose of Algorithm 1 aims to minimize the intrinsic interference rather than out of band emissions as other conventional filters.

Table 1 System simulation parameters

Parameter name	Parameter value
Modulation method	4QAM,16QAM
Number of subcarriers (M)	128
Overlap factor (K)	4
Prototype filters	NDPSS,Type1, CaseC
Filter length (L_g)	512
Filter bandwidth (B)	4, 8
Number of iterations ($i_{\max}$)	2
Threshold (γ)	0.99
Number of sequences with the highest concentration energy (N_e)	3, 25
Channel model	ITU-VB
Noise model	AWGN

The BER performance of the systems with NDPSS, Type1 and CaseC applying 4QAM modulation is depicted in Fig. 3. After observation, it is not difficult to find that compared with Type1 and CaseC, the BER performance of NDPSS is significantly improved. Meanwhile, their BER curves become very closed after one iteration, and the NDPSS curve is even close to the ideal one, which is mainly due to the fact that just like Algorithm 1, the iterative interference technique proposed in Ref. [18] limits the power of ISI below its threshold power, which has a great effect on eliminating the intrinsic interference of the FBMC-QAM system. Therefore, both of them can achieve a significant BER performance gain after one iteration.

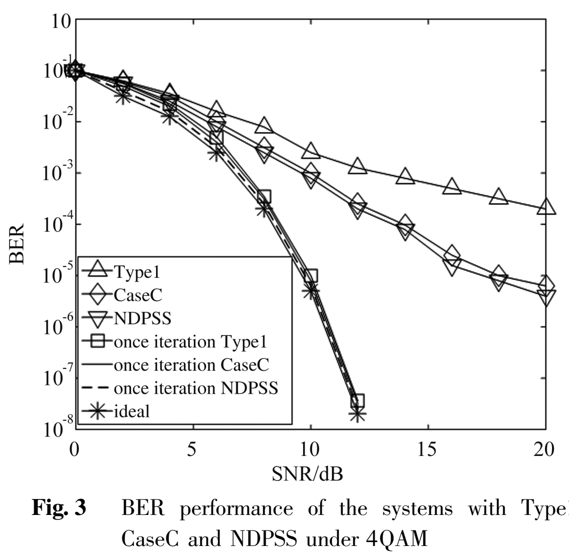

Fig. 3 BER performance of the systems with Type1, CaseC and NDPSS under 4QAM

The BER curves of them under 16QAM are illustrated in Fig. 4 and Fig. 5. According to Fig. 4, it can be found that both of their BER performances improve with the increase of iterations, and the BER performance of NDPSS is obviously better than that of Type1 under the same number of iterations, which is mainly because Algorithm 1 optimizes the weight coefficients of NDPSS during the process of two iterations, which can further mitigate its intrinsic interference. In addition, by comparing Fig. 4 with Fig. 3, it can be concluded that applying 16QAM will lead to a certain degree of BER degradation with other things being equal, the main reason lies in the fact that compared with 4QAM, 16QAM raises the transmission efficiency while deteriorating its fault tolerance.

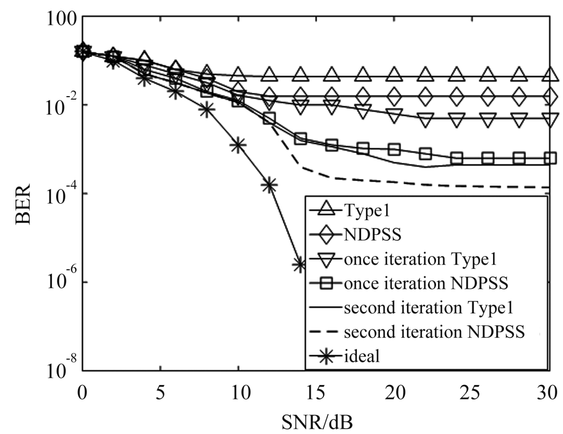

Fig. 4 BER performance of the systems with NDPSS and Type1 under 16QAM

The BER performance of them under 16QAM modulation is given in Fig. 5. It is easy to find that the BER performance of NPDSS approximately coincides with CaseC with no iteration and shows slightly better than CaseC with one iteration but exhibits a significant performance gain over CaseC after two iterations, which fully reflects the superiority of Algorithm 1.

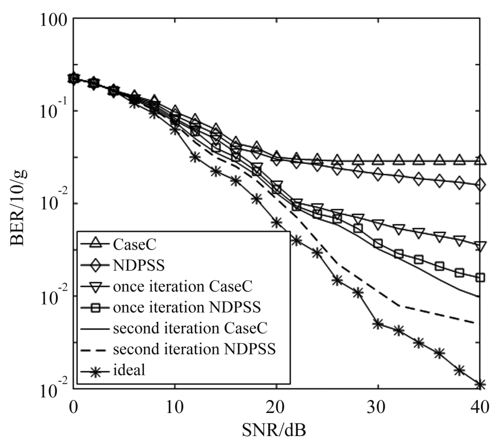

Fig. 5 BER performance of the systems with NDPSS and CaseC under 16QAM

Secondly, change the filter bandwidth and compare NDPSS with Type1 and CaseC. Suppose $B = 8$ and $N_e = 25$, therefore $p = 0, 1, \ldots, 24$, and for NDPSS it needs to optimize 25 parameters. Likewise, they have the same bandwidth but different energy distribution. Although NDPSS achieves higher attenuation at the edge of the transmission band, its passband is not smooth. The primary reason is that the NDPSS contains multiple subcarriers spaced $1/M$, which allows the interference coefficient $\Gamma_{\Delta n, \Delta k}$ to appear inside the passband of the filter during minimization.

The BER curves of three filters under 4QAM modulation are demonstrated in Fig. 6. From Fig. 6, it can be seen that the system performance of NDPSS and CaseC is relatively similar with no iteration and one iteration. It is because the global optimization algorithm of CaseC can also optimize the filter parameters as effectively as the interior point method used in Algorithm 1.

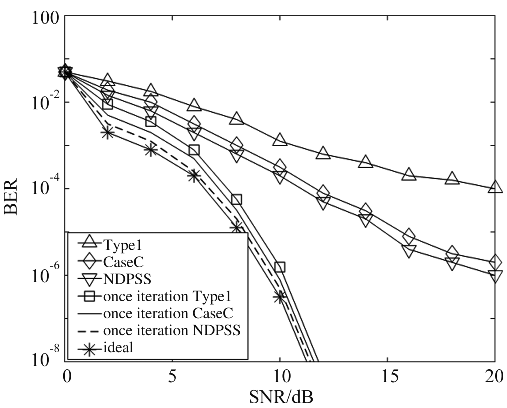

Fig. 6 BER performance of the systems with Type1, CaseC and NDPSS under 4QAM

The system BER curves for these three filters using 16QAM modulation are shown in Fig. 7 and Fig. 8. In general, the BER performance of the system deteriorates, including the filter bandwidth becoming longer and the modulation mode changing from 4QAM to 16QAM. From Fig. 7, it can be seen that changing the bandwidth of the filter does not affect the performance results of Type1 and NDPSS filters, which also proves the flexibility of NDPSS design, even if the bandwidth is changed, but still maintain good performance.

Fig. 8 depicts the system BER performance of the CaseC and NDPSS filters at 16QAM modulation. Like the comparison results under 4QAM modulation, NDPSS is still closer to the theoretical value, and different modulation methods and iteration times will indeed affect the effect of the two filters, but the NDPSS design scheme is optimized twice by the internal point method under the set threshold, which is better than the global optimization algorithm used by CaseC.

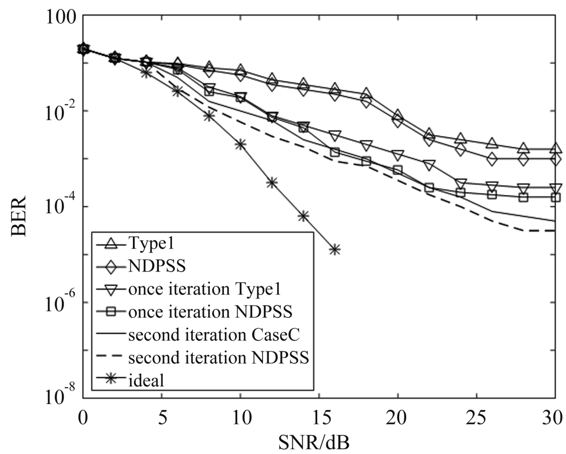

Fig. 7 BER performance of the systems with NDPSS and Type1 under 16QAM

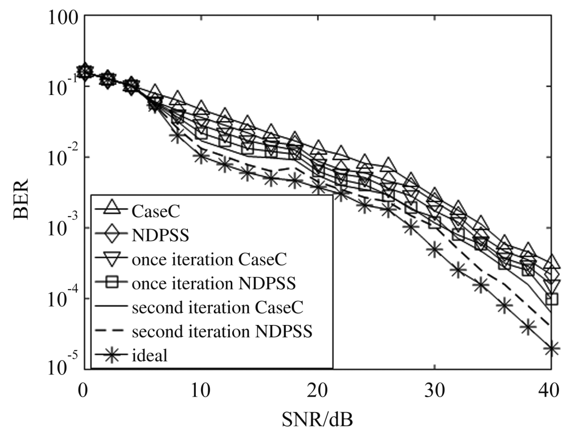

Fig. 8 BER performance of the systems with NDPSS and CaseC under 16QAM

5 Conclusions

In this paper, an NDPSS filter optimization algorithm based on the interior point method is proposed for the optimal design of the prototype filter of FBMC-QAM system. It can minimize the intrinsic interference of the FBMC-QAM system by optimizing the time-frequency parameters of the DPSS. Theoretical analysis and simulation results demonstrate that compared with Type1 and CaseC, the proposed optimization algorithm can effectively suppress the intrinsic interference in the FBMC-QAM system.

References

[1] YOU X, PAN Z, GAO X, et al. 5G mobile communication development trend and some key technologies [J]. China Science: Information Science, 2014, 44(5): 551-563.

[2] FARHANG-BOROUJENY B. OFDM versus filter bank multicarrier[J]. IEEE Signal Processing Magazine, 2011, 28(3): 92-112.
[3] CHEN D, LAN J, LUO K, et al. Symbol encryption and placement design for OQAM/FBMC systems [J]. IEEE Transactions on Communications, 2022, 70(1): 552-563.
[4] JANG T, KIM J, CHO J H. A design of spectrally-efficient low-complexity QAM-FBMC systems with mismatched prototype filters [J]. IEEE Transactions on Vehicular Technology, 2022, 71(12): 13043-13059.
[5] ANDRADE I G, RUYET D L, CAMPOS M, et al. Bit error probability expressions for QAM-FBMC systems [J]. IEEE Communications Letters, 2022, 26 (5): 994-998.
[6] GUPTA A, JHA R K. A survey of 5G network: architecture and emerging technologies[J]. IEEE Access, 2014, 3: 1206-1232.
[7] NAM H, CHOI M, HAN S, et al. A new filter bank multicarrier system with two prototype filters for QAM symbols transmission and reception [J]. IEEE Transactions on Wireless Communications, 2016, 15(9): 5998-6009.
[8] YUN Y H, KIM C, KIM K, et al. A new waveform enabling enhanced QAM-FBMC systems[C]//The 16th International Workshop on Signal Processing Advances in Wireless Communications. Stockholm, Sweden: IEEE, 2015: 116-120.
[9] KIM H, HAN H, PARK H. Waveform design for QAM-FBMC systems[C]//The 18th International Workshop on Signal Processing Advances in Wireless Communications. Sapporo, Japan: IEEE, 2017: 1-5.
[10] MOORE I C, CADA M. Prolate spheroidal wave functions, an introduction to the slepian series and its properties[J]. Applied and Computational Harmonic Analysis, 2004, 16(3): 208-230.
[11] MAHAMA S, HARBI Y J, BURR A G, et al. Iterative interference cancellation in FBMC-QAM systems [C]// Wireless Communications and Networking Conference. Marrakesh, Morocco: IEEE, 2019: 1-5.
[12] ZEMEN T, MECKLENBRAUKE C F. Time-variant channel estimation using discrete prolate spheroidal sequences [J]. IEEE Transactions on Signal Processing, 2005, 53 (9): 3597-3607.
[13] FAPING L, HONGXING W, XIAO L, et al. Time-frequency characteristics of PSWF with Wigner-ville distributions[C]// International Conference on Signal and Image Processing. Beijing: IEEE, 2016: 568-572.
[14] SAI L, LIU C, LU F, et al. A reconstructing method of PSWF pulse based on three-valued Walsh interpolation functions[C]//The 3rd Information Technology, Networking, Electronic and Automation Control Conference. Chengdu: IEEE, 2019: 271-276.
[15] OSIPOV A, ROKHLIN V, XIAO H. Prolate spheroidal wave functions order zero [M]. New York: Springer, 2013.
[16] SAHIN A, GUVENC I, ARSLAN H. A survey on multicarrier communications: prototype filters, lattice structures, and implementation aspects[J]. IEEE Communications Surveys and Tutorials, 2014, 16 (3): 1312-1338.
[17] WANG H, LU F, LIU C, et al. Frequency domain multicarrier modulation based on prolate spheroidal wave functions[J]. IEEE Access, 2020, 8: 99665-99680.
[18] Recommendation ITU-R M. 1225 Guidelines for Evaluation of Radio Transmission Technologies for IMT-2000 [S]. Geneva: International Telecommunication Union, 1997.
[19] HAN H, KWO G, PARK H. MMSE-interference canceling receiver for QAM-FBMC systems[J]. IEEE Communications Letters, 2020, 24(11): 2589-2593.

DONG Qiyang, born in 1998. He is an M. S. candidate at Shanghai University of Engineering Science. He received his B. S. degree from China Mining University in 2020. His research interests include FBMC communication technology and interference reduction technology.